UDK 004.414.23:661.834
Original scientific article/Izvirni znanstveni članek

ISSN 1580-2949
Mater. Tehnol.

CTAB-ASSISTED SYNTHESIS OF MONODISPERSE SPHERICAL $LiCO_3$ MICROCRYSTALS WITH AN ION-EXCHANGE METHOD

S CTAB PODPRTA SINTEZA HOMOGENO DISPERGIRANIH SFERIČNIH MIKROKRISTALOV $LiCO_3$ Z METODO IZMENJAVE IONOV

Zhaoyu Wu[1], Zhifu Wu[2,3,4*]

[1]School of Control Science and Engineering, Shandong University, Jinan 250002, China
[2]School of Pharmacy, Guilin Medical University, Guilin 541199, China
[3]Guangxi Key Laboratory of Drug Molecular discovery and optimization, Guilin 541199, China
[4]Engineering Research Center for Drug Molecular Screening and Drug Evaluation in Guangxi Zhuang Autonomous Region, Guilin 541199, China

Prejem rokopisa – received: 2024-11-11; sprejem za objavo – accepted for publication: 2025-01-22

doi:10.17222/mit.2024.1341

Based on modeling and optimization of the traditional reactive crystallization process, the preparation conditions of monodisperse lithium carbonate crystals and the agglomeration mechanism of the reactive crystallization process were explored in order to develop a novel multi-stage cascade crystallization process. Monodisperse Li_2CO_3 spheres were successfully fabricated with a high yield using a facile ion-exchange route in the study. In order to achieve this goal, the effects of the reactant ratio, reaction time, hexadecyl trimethyl ammonium bromide (CTAB) additive, and reaction temperature on the crystal morphology of lithium carbonate were investigated. The results revealed that the optimal experimental conditions for preparing spherical lithium carbonate are as follows: a reaction feed ratio of 1.5:1, reaction time of 9 h, reaction temperature of 85 °C, and addition of 1 % CTAB emulsifier.

Keywords: CTAB, Li_2CO_3, microcrystals, rod-like sphere

Avtorji v pričujočem članku opisujejo modeliranje in optimizacijo tradicionalnega reaktivnega kristalizacijskega procesa, pogoje priprave homogene disperzije kristalov litijevega karbonata in mehanizme aglomeracije v reaktivnem procesu kristalizacije. Avtorji so raziskavo izvedli zato, da bi razvili nov več-stopenjski kaskadni proces kristalizacije. Avtorji so uspešno izdelali homogeno disperzijo kroglic Li_2CO_3 z enostavnim visoko donosnim postopkom izmenjave ionov. Za to, da so avtorji dosegli ta cilj, so raziskovali vpliv razmerja reaktantov, reakcijski čas, dodatek cetrimonijevega bromida (CTAB; angl.: hexadecyl trimethyl ammonium bromide) in temperature reakcije na morfologijo Li_2CO_3. Rezultati raziskave so odkrili optimalne eksperimentalne pogoje za pripravo homogene disperzije krogličnih delcev Li_2CO_3 kot sledi: reakcijsko polnilno razmerje 1,5:1; reakcijski čas 9 ur; temperatura reakcije 85 °C; dodatek CTAB emulgatorja 1 %.

Ključne besede: cetrimonijev bromid (CTAB), litijev karbonat (Li_2CO_3), mikrokristali v obliki paličic in kroglic

1 INTRODUCTION

Lithium carbonate has been widely used in lithium batteries, concrete (early strength agent), cement (setting accelerator), ceramics (corrosion inhibitors for organic coatings), and drugs for mental illness treatment, as well as for metallurgical impurity removal.[1–6] In recent years, because of its high specific capacity, high energy conversion efficiency, small size, lightweight nature, long life, and environmental friendliness, lithium batteries have become an indispensable and important energy source in life, occupying a dominant position in energy storage and supply.[7–10] In addition, lithium carbonate is the first psychiatric drug to be discovered and is by far the most effective drug for the treatment of bipolar disorder, with good application prospects.[11–13]

For lithium carbonate, two main preparation methods are used. One involves smelting and extracting it from lithium ore. However, due to of the low lithium content in lithium ore, a low resource utilization rate, high energy consumption in the preparation process, and severe environmental pollution, this method of producing lithium carbonate from lithium ore is gradually being phased out. In recent years, countries around the world have been actively studying the second method of extracting lithium, i.e., extracting it from salt lake brine. Salt lake brine is prepared and extracted by evaporation concentration, lithium precipitation and drying.[14–16] The advantages of preparing lithium carbonate with this method are a simple process, easy operation, and high purity of lithium carbonate products.

With the rapid development of society and technology, people's demand for clean energy and portable and mobile energy is increasing. As a new type of energy, lithium-ion batteries are more and more important in our daily lives and industrial applications. The rapid development of the lithium battery industry makes the quan-

*Corresponding author's e-mail:
1772716011@qq.com (Zhifu Wu)

tity and quality demand for the battery-grade lithium carbonate increase. There are abundant lithium resources in salt lakes in China, with a wide distribution. This abundant lithium amount and superior geographical conditions have enabled the rapid technological production of lithium from salt lakes. Currently, precipitation,[17–20] ion-membrane separation, calcination, ion-exchange adsorption, and solar crystallization precipitation are mainly employed for producing lithium carbonate from salt lake brine.[21–25] Although the technology for the preparation of lithium carbonate has been industrialized, it is generally associated with high production costs, poor economic benefits, and low lithium carbonate yields, which affect the performance and service life of downstream products.[26]

Therefore, the reactive crystallization process of lithium carbonate from lithium chloride and sodium carbonate was studied in this work, which aimed to achieve a mass production of monodisperse battery-grade lithium carbonate crystals. Based on modeling and optimization of the traditional reactive crystallization process, the preparation conditions for monodisperse lithium carbonate crystals and the agglomeration mechanism in the reactive crystallization process were explored in order to develop a novel multi-stage cascade crystallization process. A kind of lithium chloride solution was used to simulate the lithium salt in salt lake brine to obtain rod-like and spherical lithium carbonate. Furthermore, the effects of the additional amount of lithium chloride, reaction time, CTAB as the additive, and reaction temperature on the crystal growth and morphology of lithium carbonate were investigated. Relatively good process conditions for preparing lithium carbonate from salt lake brine were obtained.

2 EXPERIMENTAL PART

2.1 Materials

Lithium chloride ($LiCl{\cdot}H_2O$) was purchased from Nanjing Marsh Reagent Effective Company. Anhydrous sodium carbonate (Na_2CO_3) was purchased from Tianjin Kemiou Chemical Reagent Co., Ltd; CTAB was purchased from Beijing Yili Fine Chemical Co., Ltd. All chemicals were of analytical purity and used without further purification.

An electronic analytical balance (Shanghai Ohaus Instrument Co., Ltd.), an electric heating blast drying oven (Shanghai Yiheng Scientific Instrument Co., Ltd.), a box-type resistance furnace (Shenyang Energy Saving Electric Furnace Factory) and a vacuum dryer (Shanghai Suopu Instrument Co., Ltd.) were used in the preparation process. X-ray diffraction (XRD) patterns were recorded on an UItima III diffractometer (Japan Rigaku Corporation) with Cu-K_α radiation at a scanning speed of 4°/min from 10° to 70°. A field emission scanning electron microscope (FE-SEM) was used on a SU-5000 (Hitachi, Japan). Transmission electron microscope analysis was conducted with a JEOL, JEM2100PLUS (Japan Electronics Co., Ltd.) microscope operating at 200 kV. Samples were dispersed in ethanol and deposited on Cu grids prior to observation. The particle size and particle size distribution were examined on laser particle size analyzing equipment (Mastersizer 2000, England).

2.2 Methods

All the reagents used in the experiments were of the analytical grade and used without further purification. In a typical synthesis, 0.4 mol/L $LiCl{\cdot}H_2O$ and 0.2 mol/L Na_2CO_3 in appropriate molar ratios were dissolved in 50 mL deionized water. 1% CTAB was added with continuous stirring, and then the mixture was transferred into a Teflon-lined stainless steel autoclave with a capacity of 60 mL. Finally, the autoclave was sealed and maintained at 85 °C for 5 h, after which it was cooled to room temperature naturally. The precipitate was collected by centrifugation, washed several times with deionized water and ethanol, and then dried in an oven at 80 °C for 5 h. Thus, the product was obtained. For the content determination, the method of Chinese Pharmacopoeia Part 2 was adopted.[27] About 1 g of this product was taken and precisely weighed. 50 mL of water and 50 mL of precise sulfuric acid titration solution (0.5 mol/L) were added. The mixture was boiled slowly to remove carbon dioxide. Then it was cooled. Phenolphthalein indicator solution was added and titrated with a sodium hydroxide standard solution (1 mol/L) Titration results were corrected with a blank test. Then 1 mL sulfuric acid solution (0.5 mol/L) was equivalent to 36.95 mg $LiCO_3$. The product conformed to the national standard GB/T11075-2013.[28]

3 RESULTS AND DISCUSSION

3.1 Phase analysis of the products

The crystallinity and phase purity of the product were characterized using XRD analysis. **Figure 1** shows the

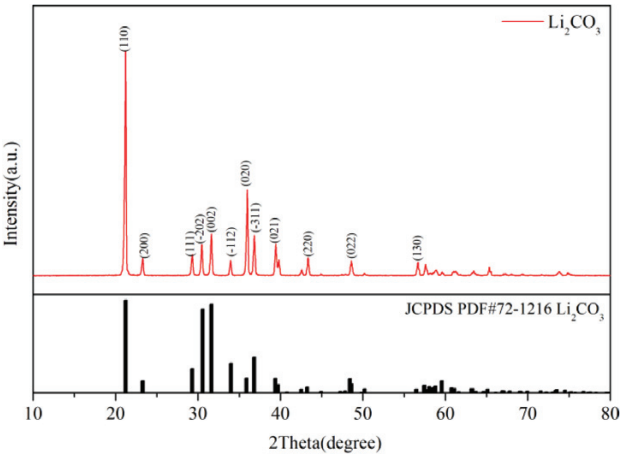

Figure 1: XRD pattern of the spherical product

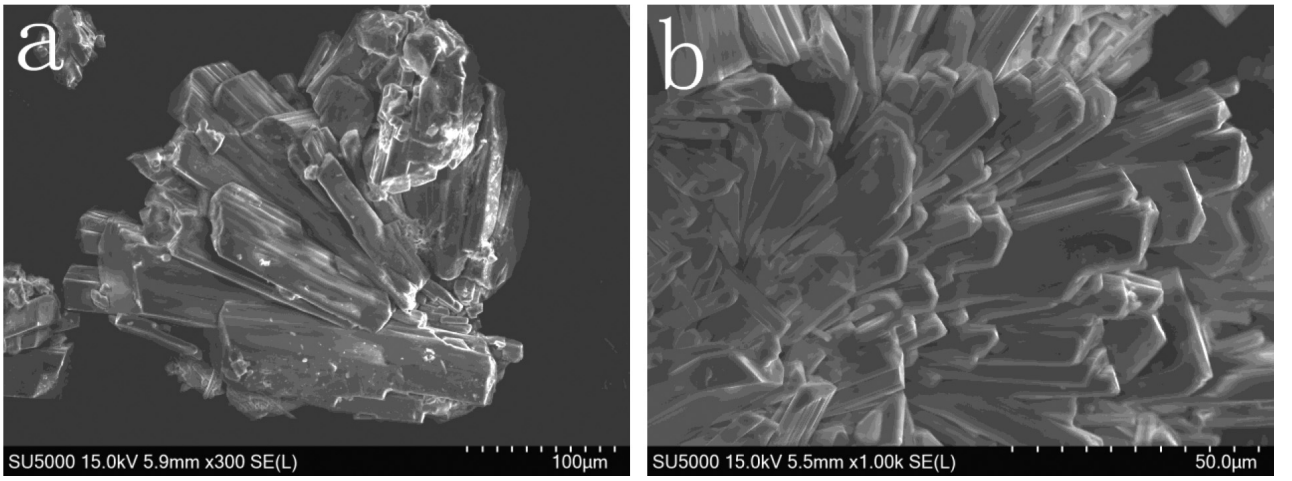

Figure 2: SEM images of the products with different amounts of lithium chloride and sodium carbonate (without CTAB) (a: 1:1, b: 1.5:1)

XRD pattern of the spherical product. Characteristic diffraction peaks are observed at 2θ values of 23.6°, 25.3°, 31.9°, 33.9°, 35.4°, and 47.6°, corresponding to those of the PDF standard card (JCPDS 72-1276),indicating that the obtained product is Li_2CO_3. No characteristic peaks of other impurities are observed, confirming the successful preparation of the pure phase.

3.2 Effect of an additional amount of lithium chloride on the crystallization of Li_2CO_3

Figure 2 shows SEM images of the product obtained at 125 °C over 6 hours. The product has a relatively regular prismatic shape. It can be seen in **Figure 2a** that at a low lithium chloride concentration, lithium carbonate crystal grains are obtained as short rods, crystal grains are relatively coarse, and some lithium carbonate crystal grains are also accompanied by coalescence. The length of the small rods is about 130–300 μm, and the diameter is about 40 μm. When the feeding ratio is 1.5:1, the grains are significantly increased, but the length and diameter of prismatic rods are basically unchanged **(Figure 2b)**. The set of experiments with a 1.5:1 ratio of lithium chloride to sodium carbonate produces more products due to the increasing lithium chloride concentration of the solution. The process is favorable to the formation of lithium carbonate crystals.

At a high lithium chloride concentration, the shape of the lithium carbonate crystal grains does not change considerably, but the crystal grain size of the lithium carbonate crystals becomes relatively small, and agglomeration is more severe. Smaller lithium carbonate crystal grains are obtained due to the degree of supersaturation caused by the increase in the lithium chloride concentration, leading to an increase in the amount of primary nucleation at the start of the reaction. As a result, lithium carbonate crystals are relatively small. The surface energy of lithium is extremely high; hence, the coalescence of lithium carbonate crystals is more severe. The severely coalesced lithium carbonate crystals are mixed with some other substances such as sodium chloride, which in turn can reduce the purity of the as-prepared lithium carbonate.

3.3 Effect of the reaction time on the crystallization yield of lithium carbonate

While maintaining other reaction conditions constant, the reaction time of lithium chloride and sodium carbonate was changed. Solutions of the same concentration and volume were prepared for four sets of experiments, and the reaction times were set to (3, 6, 9, and 12) h, respectively. Then, the obtained experimental products were dried and weighed. The lithium carbonate crystals obtained with four reaction times exhibit similar morphologies, and the particle sizes are not considerably different, which explains the reaction time at which lithium carbonate crystallizes during the reaction.

Figure 3 shows the yield-reaction time curve of the influence of reaction time on the production of lithium

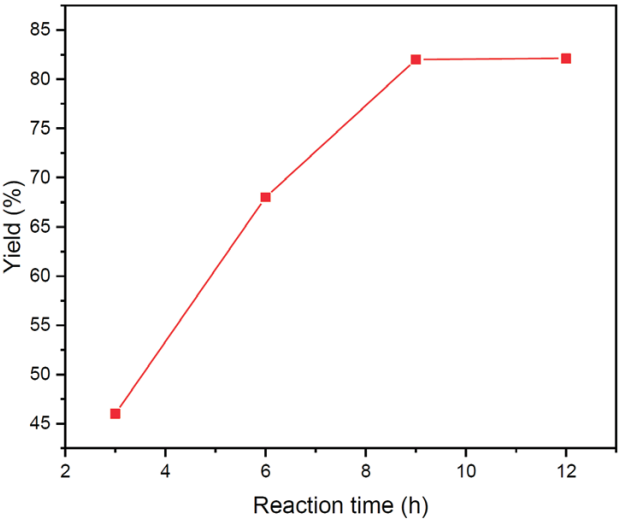

Figure 3: Schematic of the relationship between the reaction time and the yield

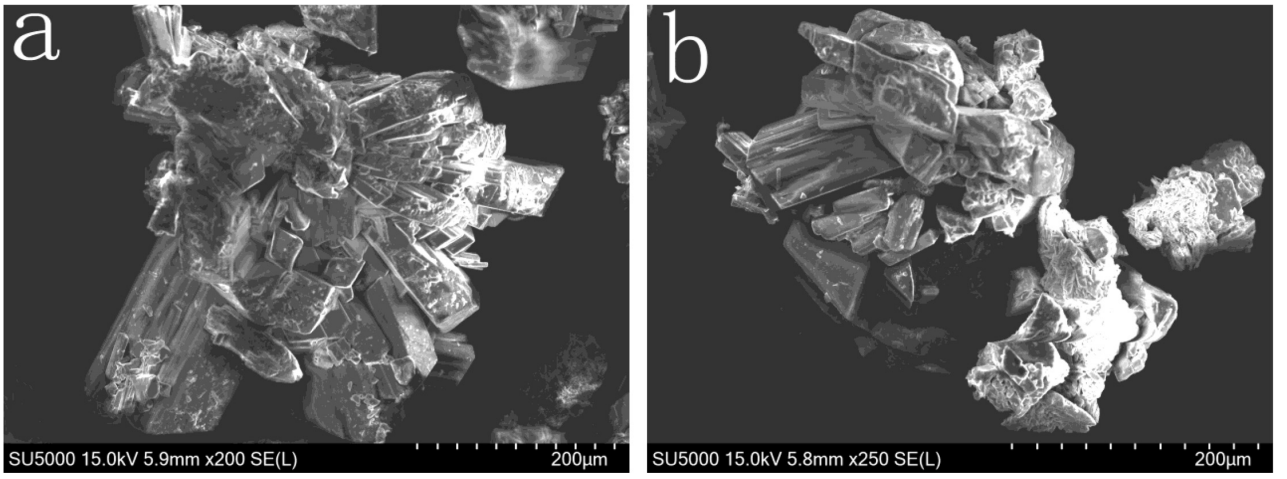

Figure 4: SEM images obtained at different reaction times (a: 3 h, b: 9 h)

carbonate. From the beginning to the reaction time within 9 h, the production of Li_2CO_3 increased with the extension of reaction time. When the reaction time was from 9 h to 12 h, the production no longer increased. Considering energy consumption and economic benefits, the optimal reaction time is 9 h. With the progress of the reaction, the yield of the obtained lithium carbonate increases, but after a certain level, it does not increase any longer. From the perspective of a chemical reaction, the solution concentration continuously decreases during the reaction. After the reactant in the solution concentration decreases to a certain level, the reaction reaches equilibrium. At this time, even if lithium chloride and sodium carbonate remain in the solution, no reaction will occur.

Figure 4 shows SEM images of the products prepared at two different reaction times (without CTAB). It can be seen from the figure that the product size is at the micrometer level. **Figure 4a** shows a SEM image of the product after a 3-h reaction, when the product shape is close to a rectangle. **Figure 4b** shows a SEM picture of the product after a 9-h reaction, when the product morphology resembles a long strip or crumb. With the change in the reaction time, the basic shape and particle size did not change; thus, the reaction time has little effect on the morphology of the product.

3.4 Effect of CTAB as an additive on the morphology of lithium carbonate

CTAB was added during the reaction, and the obtained lithium carbonate crystals were analyzed using SEM and TEM (as seen in **Figures 5** and **6**).

The surface morphology, size**,** and shape of lithium carbonate were investigated with SEM and TEM, with an addition of CTAB during the reaction, and the ratio of lithium chloride to sodium carbonate being 1:1, as shown in **Figure 5**. **Figures 5a** and **5b** show typical SEM images of the product. They present prismatic crystal grains, but the size is reduced compared with **Figures 2** and **4**.

The length of the cylinder shortened and the diameter decreased. Some grains resemble ball-cube particles of

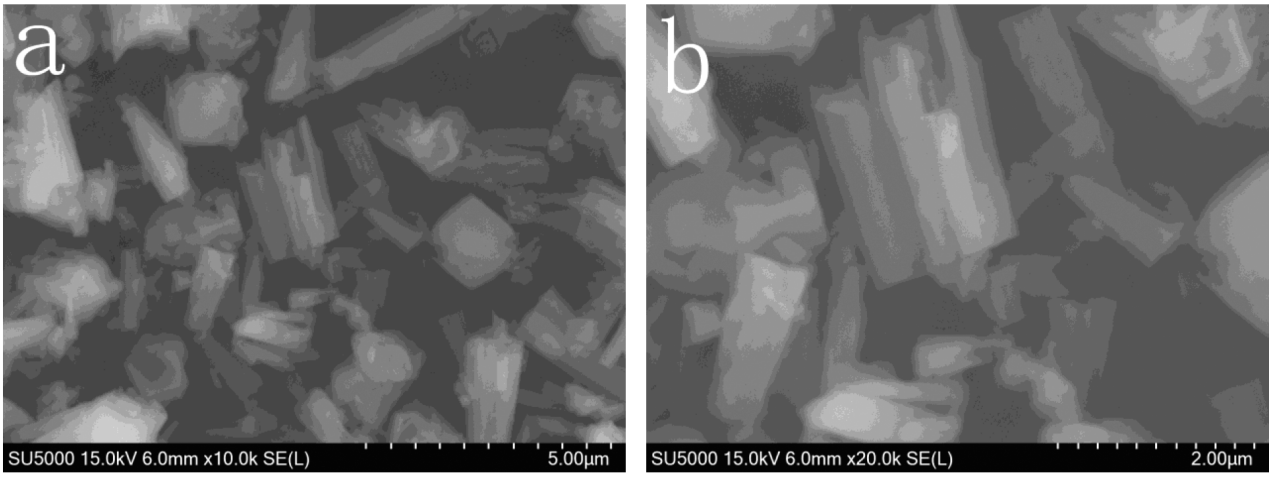

Figure 5: Morphology of the product formed after the addition of CTAB during the reaction, with the ratio of lithium chloride to sodium carbonate being 1:1

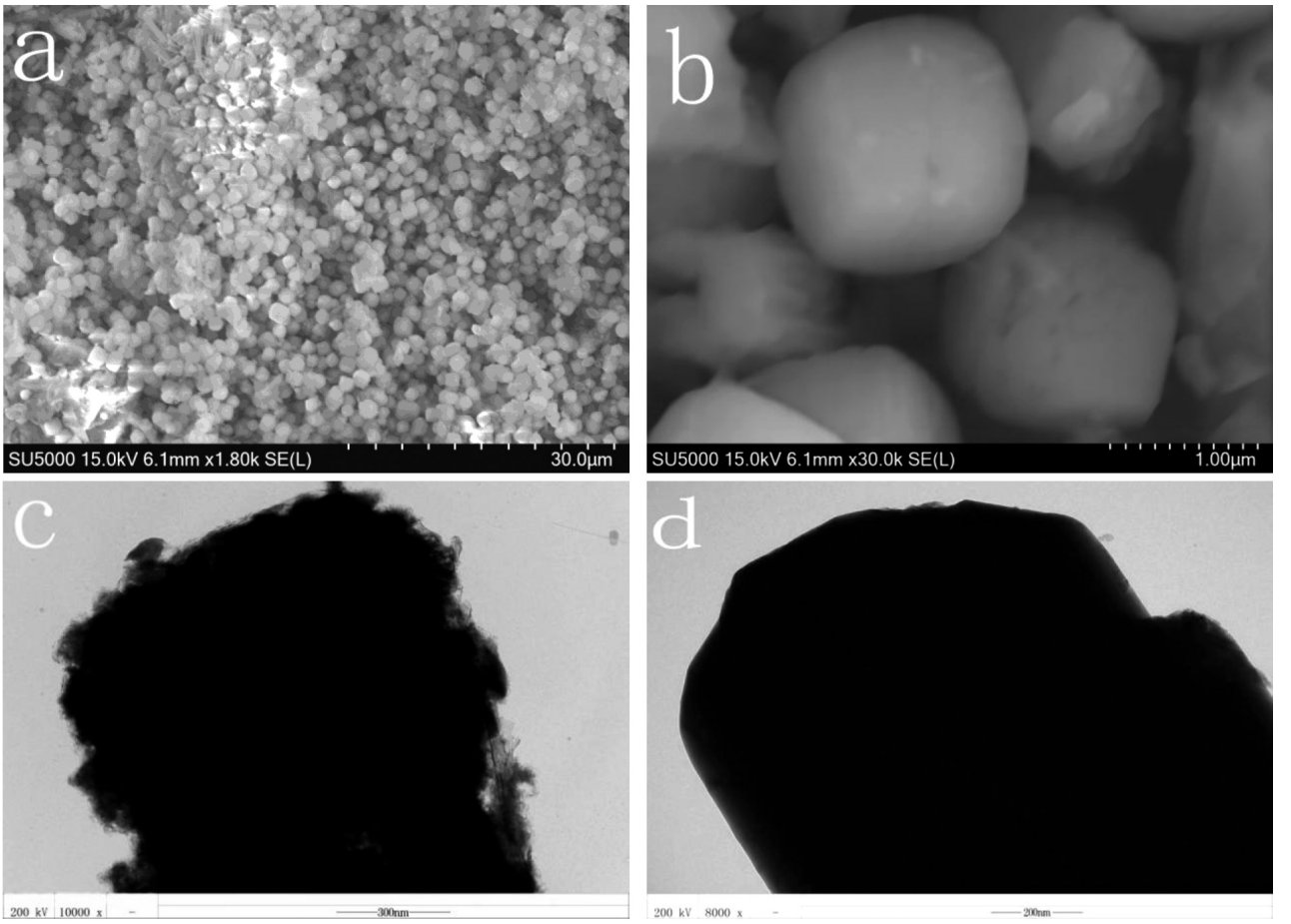

Figure 6: Morphology of the product formed with the addition of CTAB during the reaction, and the lithium chloride to sodium carbonate ratio being 1.5:1; (a, b) SEM images; (c, d) TEM images

1.5 μm to 1.7 μm in diameter, and their growth trends toward a spherical shape.

We used SEM and TEM to investigate the surface morphology, size and shape of lithium carbonate, with the addition of CTAB during the reaction, and the ratio of lithium chloride to sodium carbonate being 1.5:1, as shown in **Figure 6**. **Figures 6a** and **b** show SEM images of the product. They present uniformly dispersed spherical particles with diameters ranging from 1 μm to 1.65 μm. **Figures 6c** and **d** show TEM images of the product. It can be clearly seen that the size of a single microsphere is 1.1–1.2 μm, which is consistent with the results measured with scanning electron microscopy.

CTAB was selected as the surfactant, as it can be adsorbed on the surface of the crystal nucleus. It reduces the surface tension between the solid and liquid phases in the system and plays a role in promoting nucleation and structure orientation. Spherical lithium carbonate exhibits excellent fluidity, the surface is smooth and dense, and the performance of the final lithium carbonate product is also improved. Hence, the addition of an appropriate amount of CTAB exerts a good effect on the reaction crystallization of lithium carbonate. As a result, the optimized concentration of the CTAB dispersant in the reaction solution was found to be about 1 %.

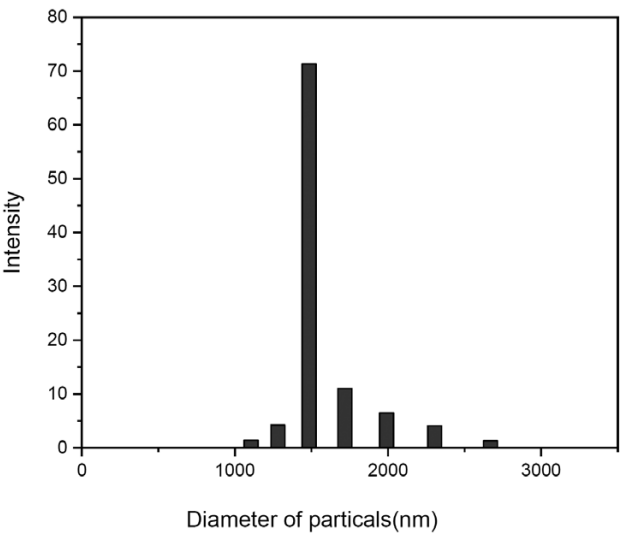

Figure 7: Particle size distribution of sphere microcrystals

3.5 Particle size distribution

The particle size and particle size distribution were examined with laser particle size analyzing equipment. **Figure 7** illustrates the particle size distribution of the as-synthesized Li_2CO_3 microspheres when the lithium chloride to sodium carbonate ratio was 1.5:1 and the reaction was kept at 85 °C for 2 h. It is obvious that the product consists of well-dispersed spherical nanoparticles with a mean diameter of 1.48 μm. The particle size distribution ranges from 1 μm to 2.6 μm.

This particle size range helps ensure the performance stability of the material in certain applications. Potential uniform dispersion and relatively concentrated particle size distribution are crucial for the application of Li_2CO_3 microspheres in fields such as battery materials. A uniform particle size enables a material to perform more stably during charging and discharging processes. Good dispersion can improve the mixing uniformity of the material with other components, thereby enhancing the overall performance of a battery.

In considering the formation mechanism of monodisperse particles originally determined by LaMer,[29] it is necessary to distinguish between two states, which often overlap, i.e., the formation of nuclei in a homogeneous environment and their subsequent growth into particles of a larger size. Monodispersed particles are favorable when the speed of nucleation is much higher than that of the particle growth.

Despite this, no particle collision occurs during the slow volatilization process, while lithium carbonate still undergoes obvious agglomeration, indicating that particle collision is not the main reason for the agglomeration of lithium carbonate. We use the LaMer model to explain and discuss its growth and formation mechanism. **Figure 8** illustrates the LaMer model of particle formation, where all nuclei initially appear instantaneously with a uniform size x, enabling a mathematical model for growth. This first theoretical attempt aims to explain how "monodisperse" particles can form. The preparation of particles with one-step oxidation requires nucleation, growth, coalescence, agglomeration and other processes. The curve qualitatively shows the variation of soluble monomer concentration vs time during the whole formation process. C_s is the saturation concentration (solubility of the soluble monomer). C_{min} is the hypothetical minimum supersaturation for the nucleation; C_{max} is the hypothetical limiting supersaturation. According to the Lamer model of crystal growth (**Figure 8**), at stage I, the reaction began to generate Li_2CO_3 solute, which accumulated, without forming a precipitate. At stage II, nucleation occurs when the concentration of the soluble monomer is higher than the critical supersaturation level C_{min}. As typically observed, Li_2CO_3 increases until the minimum supersaturation concentration required for nucleation is reached. At this point, nuclei begin to form at an effectively infinite rate, leading to "burst nucleation". When the supersaturation concentration is lower than C_{min} but higher than C_s, it enters stage III, which is the crystal growth stage by diffusion. The conditions of wet synthetic powder materials directly affect the growth of particles. According to the Gibbs-Wulff crystal equilibrium morphology, the growth rates of different crystal faces in polyhedral structures vary. Different crystal planes can modify their free energy by selectively incorporating matching ions or adsorbing surfactants, thereby promoting or inhibiting their growth. This process finally enables control of particle size and structural morphology

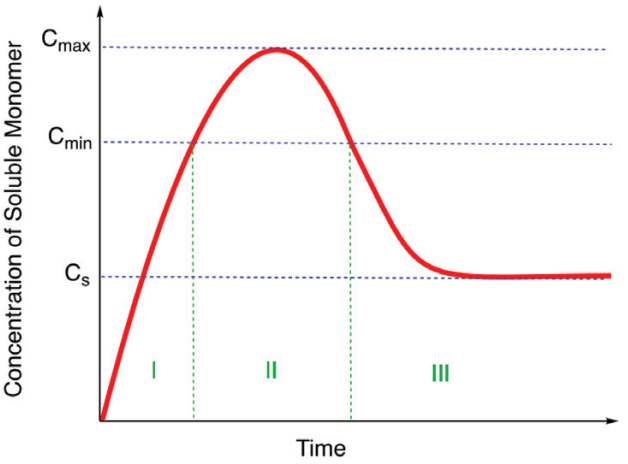

Figure 8: LaMer model of particle formation

3.6 Discussion

The above results show the effects of additives and their dosage, reaction time and reactant ratio on the experimental products. Now we shall discuss the effects of another two important reaction conditions, namely temperature and supersaturation, on the crystallization and growth of lithium carbonate. Thus, we can explore the controllable preparation conditions for monodisperse spherical lithium carbonate crystals.

3.6.1 Effect of reaction temperature on the size of lithium carbonate particles

Firstly, the influence of the chemical reaction temperature on the product conforms to the Arrhenius law, which is the most important factor affecting the quality of the product. The lithium precipitation reaction crystallization experiment was designed in a wide temperature range. Keeping the other reaction conditions constant, the reaction temperature was (45, 65, 85, and 105) °C. The crystal grain size was observed and calculated using SEM; the results are shown in **Table 1.**

Table 1: Particle size of Li_2CO_3 particles prepared at different reaction temperatures

Experimental conditions /°C	45	65	85	105
Average particle size /μm	2.0	1.8	1.5	1.6

According to the general trend shown in **Table 1,** the particle size of lithium carbonate decreases with the increase in the reaction temperature. And when the reaction temperature is 85 °C, the particle size is the smallest. This is because lithium carbonate is difficult to dissolve in water, and as the temperature increases, its solubility gradually decreases. Therefore, with the increase in the reaction temperature to 85 °C, the precipitation of lithium carbonate is more complete. The smaller the size of monodisperse spherical particles, the higher the yield. However, when the reaction temperature exceeds 85 °C, the particle size decreases again. Therefore, it is necessary to control the preparation conditions, maintaining the reaction temperature at about 85 °C. In the industrial production of lithium carbonate, the reaction temperature should be controlled to produce lithium carbonate with different crystal grain sizes.

3.6.2 Effect of supersaturation on the morphology and length-width ratio of lithium carbonate crystals

In order to investigate the effect of supersaturation on the morphology and aspect ratio of lithium carbonate crystals, the concept of supersaturation ($S = C / C_{eq}$) is used. In the formula, S is the supersaturation of lithium carbonate in the solution, C is the concentration of lithium carbonate in the solution (calculated based on the complete reaction of lithium chloride and sodium carbonate), and C_{eq} is the solubility of lithium carbonate in water. When $2 < S < 4$, lithium carbonate crystals form agglomerated rod-like crystals, and many smaller crystals are attached to the surfaces of large crystals. These fine crystals may be grown due to secondary nucleation on the surfaces of large crystals and are closely connected with the parent particles. The aspect ratio of lithium carbonate crystals follow a more distinct pattern with changes in temperature and supersaturation. In order to reduce the experimental error, the aspect ratio is obtained by averaging multiple measurements. When $S > 4$, it can be found that lithium carbonate agglomerates into spheres at higher supersaturation. With the increase in temperature and supersaturation, the size of spherical agglomerated particles is smaller and the particles are better dispersed. Monodisperse lithium carbonate crystals with well-defined morphology were obtained through instantaneous sampling.

In addition, the impurities in the solution, such as sodium chloride, potassium chloride and other impurities in industrial raw materials, also affect the morphology and coalescence of lithium carbonate crystals. The above discussion and analysis show that the preparation of monodisperse spherical lithium carbonate is very demanding in process conditions.

3.6.3 Reasonable formation mechanism for Li_2CO_3 microspheres

A plausible mechanism for the formation of Li_2CO_3 microspheres is shown in **Figure 9**.

After a dropwise addition of a LiCl aqueous solution into the $NaCO_3$/CTAB solution, a large amount of negatively charged colloidal particles with hydrated Li^+ as the compact layer is formed due to the rapid hydrolysis under a strong alkaline environment. At the beginning of the hydrothermal process, these colloidal particles are then loosely aggregated due to the surface adsorption of CTAB, followed by the formation of secondary micrometer-sized microspheres. With the increase in the reaction time, the primary colloidal particles are transformed into a mixture, but the entire particle structure is not destroyed because of the surface protection provided by CTAB. Finally, Li_2CO_3 microspheres are obtained by subsequent calcination, in which CTAB is decomposed in air.

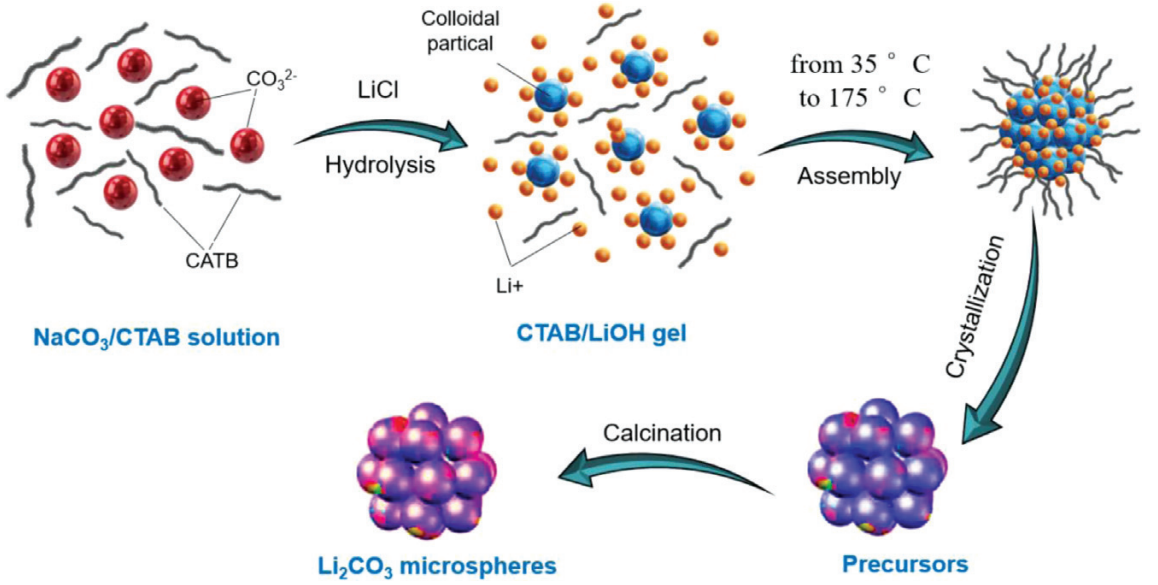

Figure 9: Reasonable formation mechanism of Li_2CO_3 microspheres

4 CONCLUSIONS

Based on the above experiments, we can conclude the following: First, the feeding ratio of reactants has a great influence on the morphology and size of the product. When lithium chloride is excessive, the grain size of lithium carbonate crystals becomes smaller and the number of lithium carbonate crystals increases, leading to a higher yield. Second, the reaction time has little effect on the grain morphology and size of lithium carbonate, but selecting the appropriate reaction time can reduce the production costs. Third, the CTAB additive has a significant influence on the morphology and size of lithium carbonate crystals. When the amount of lithium chloride is appropriate, the original coalescence transforms into dispersed short rods and finely broken cubes. When the amount of lithium chloride is excessive, the morphology of lithium carbonate changes from coalesced short rods to uniform and dispersed spherical particles. Fourth, the reaction temperature mainly affects the particle size of crystallized lithium carbonate. The experiment shows that with an increase in the reaction temperature, the particle size of lithium carbonate crystals tends to decrease. Finally, the optimal experimental conditions for preparing spherical lithium carbonate are as follows: a reaction feed ratio of 1.5:1; a reaction time of 9 h; a reaction temperature of 85 °C; and an addition of 1 % of CTAB.

5 REFERENCES

[1] H. Han, Z. Zhang, Y. C. Zou, K. Xu, G. Y. Xu, H. Wang, H. Meng, Y. H. Deng, J. Li, M. Gu, Poor stability of Li_2CO_3 in the solid electrolyte interphase of a lithium-metal anode revealed by cryo-electron microscopy, Adv. Mater., 33 (**2021**) 22, 2100404, doi:10.1002/adma.202100404

[2] J. Q. Gong, W. Guo, X. Gong, Y. Zhang, Z. L. Xie, W. X. Wu, Y. F. Dai, Effects of lithium carbonate and nano-calcium carbonate on early mechanical properties of UHPC, J. Chin. Ceram. Soc., 39 (**2020**) 11, 3464–3472, doi:10.16552/j.cnki.issn1001-1625.2020.11.010

[3] J. Sun, L. Ye, X. Zhao, P. Zhang, J. Yang, Electronic modulation and structural engineering of carbon-based anodes for low-temperature lithium-ion batteries: A review, Molecules, 28 (**2023**), 2108, doi:10.3390/molecules28052108

[4] A. J. Smith, S.-H. Kim, J. Tan, K. B. Sneed, P. R. Sanberg, C. V. Borlongsan, R. D. Shytle, Plasma and brain pharmacokinetics of previously unexplored lithium salts, RSC. Adv., 4 (**2014**) 24, 12362–12365, doi:10.1039/C3RA46962J

[5] A. G. Pacholko, L. K. Bekar, Lithium orotate: A superior option for lithium therapy? Brain and Behavior, 11 (**2021**) 8, 2262, doi:10.1002/brb3.2262

[6] R. M. Demirer, S. Kesebir, The entropy of chaotic transitions of EEG phase growth in bipolar disorder with lithium carbonate, Sci. Rep., 11 (**2021**) 1, 1–11, doi:10.1038/s41598-021-91350-9

[7] G. Wen, L. Tan, X. X. Lan, H. Y. Zhang, R. Z. Hu, B. Yuan, L. Liu, M. Zhu, Li_2CO_3 induced stable SEI formation: An efficient strategy to boost reversibility and cyclability of Li storage in SnO_2 anodes, Sci. China Mater., 64 (**2021**) 5, 1–14, doi:10.1007/s40843-021-1665-1

[8] Y. Feng, C. Y. Cao, J. Zeng, R. C. Wang, B. Yuan, L. Liu, M. Zhu, Hierarchical porous Co_3O_4 spheres fabricated by modified solvothermal method as anode material in Li-ion batteries, Trans. Nonferrous Met. Soc. China, 32 (**2022**), 1253-1260, doi:10.1016/S1003-6326(22)65871-0

[9] J. Yan, W. F. Liu, C. Chen, C. H. Zhao, K. Y. Liu, Synthesis and characterization of porous monodisperse carbon spheres/selenium composite for high-performance rechargeable Li-Se batteries, Trans. Nonferrous Met. Soc. China, 28 (**2018**), 1819-1827, doi:10.1016/S1003-6326(18)64826-5

[10] S. Ma, Z. Zhang, Y. Wang, Z. J. Yu, C. Cui, M. X. He, H. Huo, G. P. Yin, P. J. Zuo, Iodine-doped sulfurized polyacrylonitrile with enhanced electrochemical performance for lithium sulfur batteries in carbonate electrolyte, Chem. Eng. J., 418 (**2021**), 129410, doi:10.1016/j.cej.2021.129410

[11] S. Mosolov, C. Born, H. Grunze, Electroconvulsive therapy in bipolar disorder patients with ultra-rapid cycling and unstable mixed states, Medicina, 57 (**2021**) 6, 624, doi:10.3390/medicina57060624

[12] M. L. Gregório, G. L. L. Wazen, A. H. Kemp, J. C. Milan-Mattos, A. Porta, A. M. Catai, M. F. Godoy, M. F. De Godoy, Non-linear analysis of the heart rate variability in characterization of manic and euthymic phases of bipolar disorder, J. Affec. Disord., 275 (**2020**), 136–144, doi:10.1016/j.jad.2020.07.012

[13] J. K. Rybakowski, Response to lithium in bipolar disorder: clinical and genetic findings, ACS Chem. Neurosci., 5 (**2014**) 6, 413–421, doi:10.1021/cn5000277

[14] S. Klein, S. Van Wickeren, S. Röser, P. Bärmann, K. Borzutzki, B. Heidrich, M. Börner, M. Winter, T. Placke, J. Kasnatscheew, Understanding the outstanding high-voltage performance of NCM523|| graphite lithium ion cells after elimination of ethylene carbonate solvent from conventional electrolyte, Adv. Ener. Mater., 11 (**2021**) 14, 2003738, doi:10.1002/aenm.202003738

[15] J. F. Song, L. D. Nghiem, X.-M. Li, T. He, Lithium extraction from Chinese salt-lake brines: opportunities, challenges, and future outlook, Environ. Sci. Water Res. Techn., 3 (**2017**) 4, 593–597, doi:10.1039/C7EW00020K

[16] S. Gu, S. W. Zhang, J. Han, Y. Deng, C. Luo, G. Zhou, Y. He, G. Wei, F. Kang, W. Lv, Q. H. Yang, Nitrate Additives Coordinated with Crown Ether Stabilize Lithium Metal Anodes in Carbonate Electrolyte, Adv. Funct. Mater., 31 (**2021**) 28, 2102128, doi:10.1002/adfm.202102128

[17] M. Ohyama, S. Kudo, S. Amari, H. Takiyama, Production of crystalline particles with high homogeneity in reaction crystallization by using pH-solubility-profile, J. Indus. Eng. Chem., 75 (**2019**), 38–43, doi:10.1016/j.jiec.2019.03.003

[18] J. C. Kelly, M. Wang, Q. Dai, O. Winjobi. Energy, greenhouse gas, and water life cycle analysis of lithium carbonate and lithium hydroxide monohydrate from brine and ore resources and their use in lithium ion battery cathodes and lithium ion batteries, Resourc. Conser. Recy., 174 (**2021**), 105762, doi:10.1016/j.resconrec.2021.105762

[19] W. Xu, D. Liu, L. He, Z. Zhao, A Comprehensive Membrane Process for Preparing Lithium Carbonate from High Mg/Li Brine, Membranes, 10 (**2020**) 12, 371, doi:10.3390/membranes10120371

[20] A. Kosari, F. Tichelaar, P. Visser, H. Zandbergen, H. Terryn, J. M. C. Mol, Laterally-resolved formation mechanism of a lithium-based conversion layer at the matrix and intermetallic particles in aerospace aluminium alloys, Corro. Sci., 190 (**2021**), 109651, doi:10.1016/j.corsci.2021.109651

[21] J. Wei, M. Zhang, Y. Wang, S. Qiao, H. Zhang, X. Li, Synergistic optimization of thermoelectric performance in cementitious composites by lithium carbonate and carbon nanotubes, Inter. J. Ener. Res., 45 (**2021**) 2, 2460–2473, doi:10.1002/er.5940

[22] C. Liang, S. Liang, Y. Xia, Y. Gan, L. Fang, Y. Jiang, X. Tao, H. Huang, J. Zhang, W. Zhang, Synthesis of hierarchical porous carbon from metal carbonates towards high-performance lithium storage, Green Chem., 20 (**2018**) 7, 1484–1490, doi:10.1039/C7GC02841E

[23] J. Zhao, Y. Wang, High-capacity full lithium-ion cells based on nanoarchitectured ternary manganese–nickel–cobalt carbonate and its lithiated derivative, J. Mater. Chem. A., 2 (**2014**) 36, 14947–14956, doi:10.1039/C4TA02574A

[24] D.-W. Kim, S. Y. Kim, K. S. Yang, Synthesis of freestanding binder- and additive-free carbon nanofiber with graphene-wrapped Nb_2O_5 composite anode for lithium-ion batteries, Nanotechnology, 33 (**2021**) 1, 015602, doi:10.1088/1361-6528/ac162d

[25] Y. Gao, M. Zhai, Y. Sui, D. Li, W. Wang, Multifunctional polyimides containing triarylamine for electrochromic flexible device, photodetector and resistance memory device, Multifunctional Mater., 4 (**2021**) 3, 34002, doi:10.1088/2399-7532/ac150a

[26] P. Jia, M. Yu, X. Zhang, T. Yang, D. Zhu, T. Shen, L. Zhang, Y. Tang, J. Huang, In-situ imaging the electrochemical reactions of Li-CO_2 nanobatteries at high temperatures in an aberration corrected environmental transmission electron microscope, Nano Res., 15 (**2022**), 542–550, doi:10.1007/s12274-021-3514-9

[27] J. G. Li, X. D. Sun, H. Q. Ru, S. M. He, Wet chemical principles of monodisperse ultrafine ceramic powders, J. Funct. Mater., 4 (**1997**), 1–4

[28] National Pharmacopoeia Commission, Pharmacopoeia of the People's Republic of China, Part 2, 11th ed., China Pharmaceutical Science and Technology Press, Beijing 2020, 1503

[29] GB/T 23853-2022, General Administration of Market Supervision, Lithium Carbonate Made of Brine, State Standardization Administration, National Standards of the People's Republic of China